Electronic Supporting Information

Morphology evolution via solvent optimization enables all-polymer solar cells with improved efficiency and reduced voltage loss

Zhenye Li[a,b], Feng Peng[a,c,*], Xitang Qian[b], Jingwen Li[a], Zhiming Zhong[a,c], Lei Ying[a,c,*], Hongbin Wu[a], Fei Huang[a,c], and Yong Cao[a]

[a] Institute of Polymer Optoelectronic Materials and Devices, State Key Laboratory of Luminescent Materials and Devices, South China University of Technology, Guangzhou 510640, China

[b] College of Mechanical Engineering, University of South China, Hengyang 421001, China

[c] South China Institute of Collaborative Innovation, Dongguan 523808

Corresponding authors

pengfeng2012@163.com (F. Peng)

msleiying@scut.edu.cn (L. Ying)

Experimental Section

Materials

PFA1 was synthesised according to procedures reported in the literature.[1] Poly[(2,6-(4,8-bis(5-(2-ethylhexyl)thiophen-2-yl)-benzo[1,2-b:4,5-b']dithio-phene))-alt-(5,5-(1',3'-di-2-thie nyl-5',7'-bis(2-ethylhexyl)benzo[1',2'-c:4',5'-c']dithiophene-4,8-dione)] (PBDB-T) was purchased from 1-Material. Chlorobenzene (CB), chloroform (CF) and 1-chloronaphthalene (CN) are purchased from Sigma-Aldrich without further purification.

Fabrication of Polymer Solar Cells

Indium tin oxide (ITO)-coated glass substrates were successively cleaned by sonication in detergent, deionised water, acetone, and isopropyl alcohol and dried in an oven at 85 °C for 12 h prior to use. The ITO-coated glass substrates were then exposed to oxygen plasma for 5 min and spin coated with PEDOT:PSS (Clevios P VP Al 4083) at 3000 rpm for 30 s to produce 40-nm thin films. The coated substrates were annealed at 150 °C on a hot plate for 10 min. After that, they were transferred to a glove box under N_2 atmosphere. For CF processed all-PSCs, the total concentration of PBDB-T:PFA1 (1:1) was fixed at 10 mg mL^{-1}, and the blend films were obtained by spin coating solutions of PBDB-T:PFA1 (1:1) in CF containing CN (1 vol %). For CB processed all-PSCs, the total concentration of PBDB-T:PFA1 (1:1) was fixed at 12 mg mL^{-1}, and the blend films were obtained by spin coating solutions of PBDB-T:PFA1 (1:1) in CB containing CN (1 vol %). The PBDB-T:PFA1 (1:1) films were then thermally annealed at 100 °C for 10 min, followed by spin coating of a 5-nm layer of PFN-Br at 2000 rpm for 30 s to serve as the cathode interface. A 100-nm argentum (Ag) layer was then thermally deposited onto the PBDB-T:PFA1 (1:1) films by a shadow mask in a vacuum chamber with a base pressure of 2×10^{-6} mbar. The effective area of the PBDB-T:PFA1 devices was determined to be 0.0516 cm^2 by the shadow mask.

Fabrication and Characterisation of Charge-Only Devices

The hole mobility of PBDB-T:PFA1 films processed by CF and CB was measured in a hole-only device with the configuration of ITO/PEDOT:PSS/PBDB-T:PFA1/Ag. The electron mobility of PBDB-T:PFA1 films processed by CF and CB was measured in an electron-only device with the configuration of ITO/ZnO/PBDB-T:PFA1/PFN-Br/Ag. The ZnO sol-gel is obtained from stirring the solution of 2.0 g Zn(CH3COO)2·2H2O in 20 mL ethylene glycol monomethyl ether and 550 μL ethylenediamine at 50 °C for 24 h. For CF processed all-PSCs, the total concentration of PBDB-T:PFA1 (1:1) was fixed at 10 mg mL^{-1}, and the blend films were obtained by spin coating solutions of PBDB-T:PFA1 (1:1) in CF containing CN (1 vol %). For CB processed all-PSCs, the total concentration of PBDB-T:PFA1 (1:1) was fixed at 12 mg mL^{-1}, and the blend films were obtained by spin coating solutions of PBDB-T:PFA1 (1:1) in CB containing CN (1 vol %). The mobility μ of PBDB-T:PFA1 films processed by CF and CB was determined by fitting the dark current to the model of a single-carrier SCLC, which is described by Equation (1):

$$J = (9/8)\varepsilon_0 \varepsilon_r \mu V_{eff}^{\,2}/d^3, \tag{1}$$

where J is the current density of PBDB-T:PFA1 device, μ is the hole or electron mobility at zero field, ε_0 is the permittivity of free space, ε_r is the relative permittivity of the polymers, d is the thickness of the PBDB-T:PFA1 layer, and V_{eff} is the effective voltage ($V-V_{bi}$) of PBDB-T:PFA1 device. The hole or electron mobility was calculated from the y intercept of the J–V curves of PBDB-T:PFA1 device.

Instruments and Characterisation

The number-average molecular weight (M_n) and polydispersity index (PDI) of PFA1 was determined on a Polymer Laboratories PL-GPC 220 using 1,2,4-trichlorobenzene as the eluent at 150 °C vs. polystyrene standards. The absorption spectra of PBDB-T:PFA1 films processed

by CF and CB were measured using a UV–vis spectrophotometer (HP 8453, photodiode array type) in the wavelength range of 300-1000 nm. The electrochemical cyclic voltammetry experiments were conducted on a CHI600D electrochemical workstation with a platinum working electrode and a Pt wire counter electrode at a scanning rate of 50 mV s^{-1} against an Ag/Ag$^+$ (0.1 M of AgNO$_3$ in acetonitrile) reference electrode with a nitrogen-saturated anhydrous solution of 0.1 mol L^{-1} tetrabutylammonium hexafluorophosphate in acetonitrile. The current density–voltage (J–V) characteristics of PBDB-T:PFA1 devices processed by CF and CB were measured using a computer-controlled Keithley 2400 SourceMeter under 1 sun irradiation from an AM 1.5 G solar simulator (Taiwan, Enlitech, SS-F5). The EQE spectra of PBDB-T:PFA1 devices processed by CF and CB were measured using a commercial EQE system (Taiwan, Enlitech, QE-R3011). AFM images were obtained by using a Bruker Multimode 8 Microscope AFM in tapping-mode. Transmission electron microscopy images were collected from a JEM-2100F transmission electron microscope operated at 200 kV. PL spectra were recorded on a Jobin-Yvon FluoroMax-4 spectrofluorometer. GIWAXS characterization was performed at State Key Laboratory of Luminescent Materials and Devices, South China University of Technology.

Grazing incidence wide-angle X-ray scattering (GIWAXS)

A 10 keV energy was employed as the X-ray beam energy. Thin PBDB-T:PFA1 film samples were obtained by spin-coating their solution in CF or CB on PEDOT:PSS/silicon substrates. The detector distance of PBDB-T:PFA1 films processed by CF and CB was ~214 mm. Each GIWAXS signal was recorded in Helium atmosphere with exposure time of 5 s, where a 2D charge-coupled device (CCD) detector (Pilatus 2M) with a pixel size of 0.172 mm by 0.172 mm was used.

Transient photocurrent (TPC) measurements

The PBDB-T:PFA1 devices processed by CF and CB were excited with a 405 nm laser diode. Removing background lighting, the PBDB-T:PFA1 device responds to a 200 μs square wave from the LED in a transient photocurrent response under short-circuit conditions. The current trace was then recorded on a Tektronix DPO3034 digital oscilloscope by measuring the voltage drop across the 5-ohm sensor resistance in series with the PBDB-T:PFA1 device. The MRF544 bipolar junction transistor with a common collector amplifier is employed to apply a DC voltage to the device.

Transient photovoltage (TPV) measurements

The PBDB-T:PFA1 devices processed by CF and CB were linked to the oscilloscope under open circuit conditions (1MΩ), and then the devices were illuminated with white LEDs at different light intensities. After that, a 405 nm laser diode was employed to form a small optical disturbance by adjusting the light intensity to produce a voltage disturbance. The amount of generated charge by the pulse comes from integrating the unpolarized photocurrent measurement value (50Ω).

Fourier-transform photocurrent spectroscopy external quantum efficiency (FTPS-EQE) and electroluminescence (EL) measurement

The highly sensitive FTPS-EQE of PBDB-T:PFA1 devices processed by CF and CB was measured using a Vertex 70 from Bruker Optics (equipped with a quartz tungsten halogen lamp, quartz beamsplitter and external detector option). After that, a low-noise current amplifier (SR570) was employed to amplify the generated photocurrent under illumination of the PBDB-T:PFA1 device, with Fourier transform infrared spectroscope (FTIR) modulating the light. The output voltage of the current amplifier was fed back into the external detector port of the FTIR, so that the FTIR software can collect the photocurrent spectra. The EQE_{EL} of PBDB-T:PFA1 devices processed by CF and CB was recorded with an in-house-built

system, which is comprised of a Hamamatsu silicon photodiode 1010B, Keithley 2400 source meter, and Keithley 485 picometer.

Additional Figures and Tables

Table S1. Optical and electrical properties of PFA1.

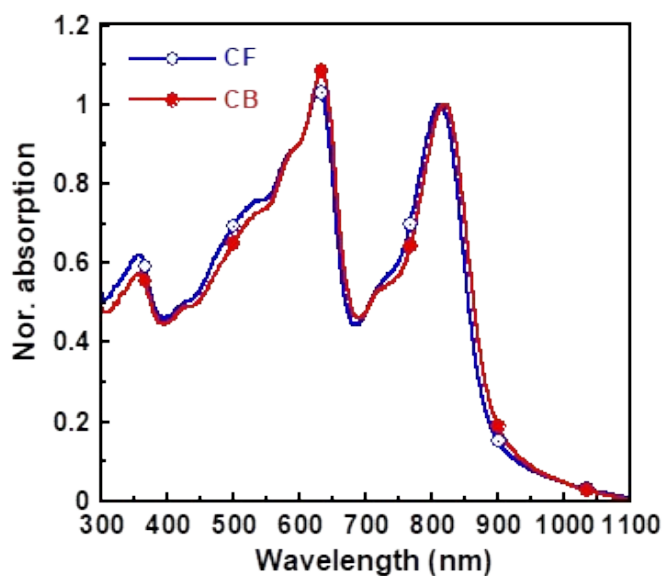| Polymer	E_{HOMO} (eV)	E_{LUMO} (eV)	M_w (kg mol^{-1})	M_n (kg mol^{-1})	PDI
PFA1	-5.74	-3.84	31.4	13.4	2.34

Fig. S1. UV-vis-NIR absorption spectra of PBDB-T:PFA1 films processed by CF and CB.

Table S2. Solubility of PBDB-T and PFA1 in various solvent.

Solvent	PBDB-T (mg mL^{-1})	PFA1 (mg mL^{-1})
CF	36	45
CB	27	35

Table S3. Photovoltaic parameters of all-PSCs based on PBDB-T:PFA1 devices processed by various solvent.

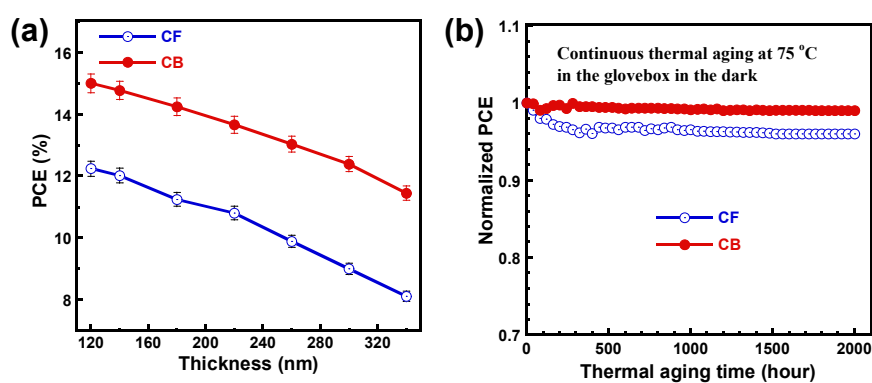| Solvent	V_{OC} (V)	J_{SC} (mA cm^{-2})	FF (%)	PCE (%)
DCB	0.84	23.56	70.68	13.99
THF	0.80	15.68	60.25	7.56
Toluene	0.81	21.96	68.85	12.25

Fig. S2. PCE versus thickness characteristics (a) and normalized PCE during continuous thermal aging in the glovebox at 75 °C in the dark (b) of PBDB-T:PFA1 devices processed by CF and CB.
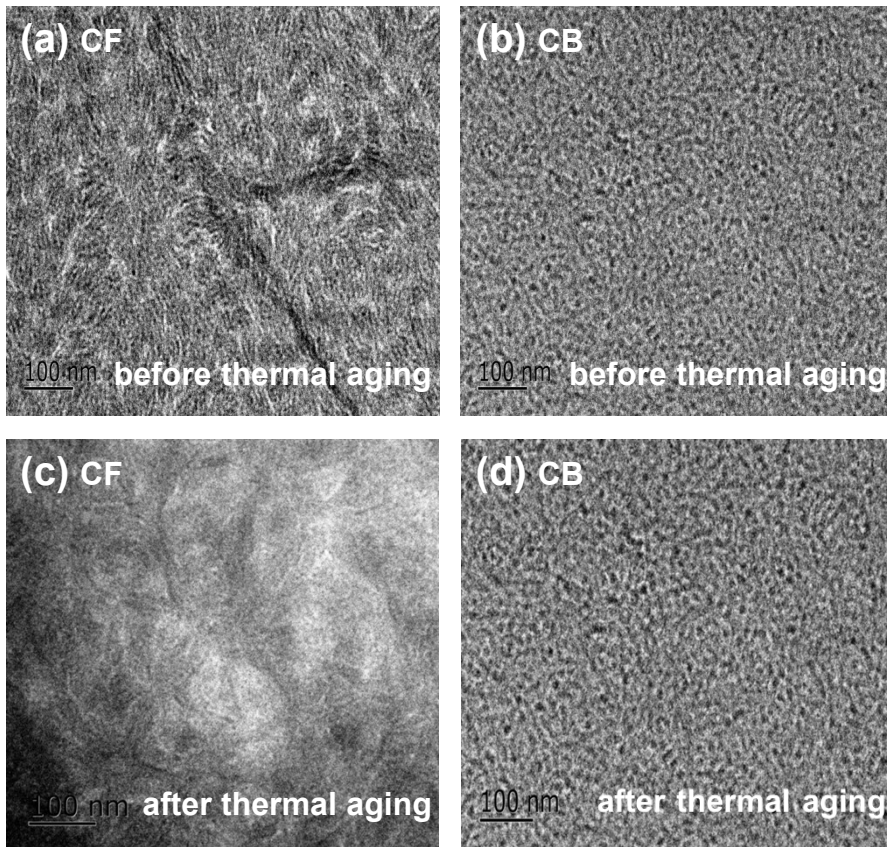
Fig. S3. TEM images of PBDB-T:PFA1 films processed by CF (a) and CB (b) before thermal aging; TEM images of PBDB-T:PFA1 films processed by CF (a) and CB (b) after thermal aging for 200 h.
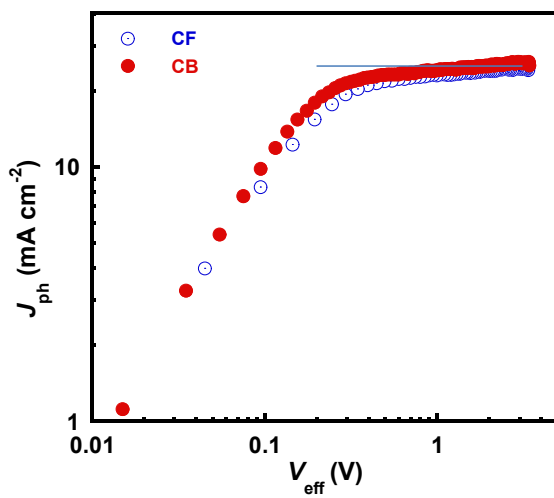

**Fig. S4.** $J_{ph}-V_{eff}$ curves for PBDB-T:PFA1 devices processed by CF and CB.

Table S4. Relevant parameters obtained from J_{ph}–V_{eff} curves.

Active layer [a]	J_{ph} [b] (mA cm^{-2})	J_{sat} (mA cm^{-2})	G_{max} (m^{-3} s^{-1})	$P(E, T)$ [b]	L (nm)
CF	22.94	24.52	1.47×10^{28}	0.936	~120
CB	23.96	25.80	1.55×10^{28}	0.929	~120

[a] All of the blend films were treated with 100 °C for 10 min ; [b] At the condition of $V_{eff} = V_0 - V_{appl}$ ($V_{appl} = 0$, under short-circuit condition).

Table S5. SCLC electron (hole) mobility measurements for neat PBDB-T, neat PFA1 and PBDB-T:PFA1 films processed by CF and CB.

Active layer	μ_h (cm^2 V^{-1} s^{-1})	μ_e (cm^2 V^{-1} s^{-1})	μ_h/μ_e	Thickness (nm)
PBDB-T:PFA1 by CF	3.12×10^{-4}	1.48×10^{-4}	2.11	~120
PBDB-T:PFA1 by CB	3.92×10^{-4}	3.62×10^{-4}	1.08	~120
PBDB-T by CF	0.99×10^{-3}	/	/	~120
PBDB-T by CB	1.10×10^{-3}	/	/	~120
PFA1 by CF	/	5.21×10^{-4}	/	~120
PFA1 by CB	/	8.37×10^{-4}	/	~120
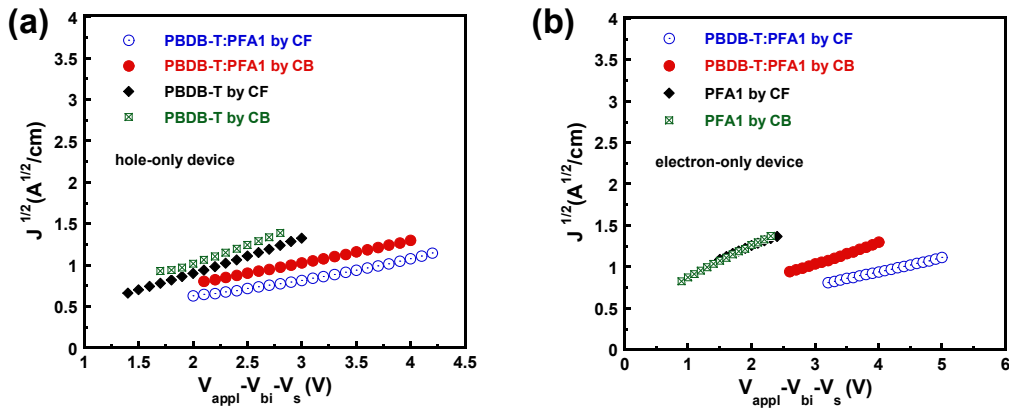
Fig. S5. SCLC hole (a) and electron (b) mobility for neat PBDB-T, neat PFA1 and PBDB-T:PFA1 films processed by CF and CB.
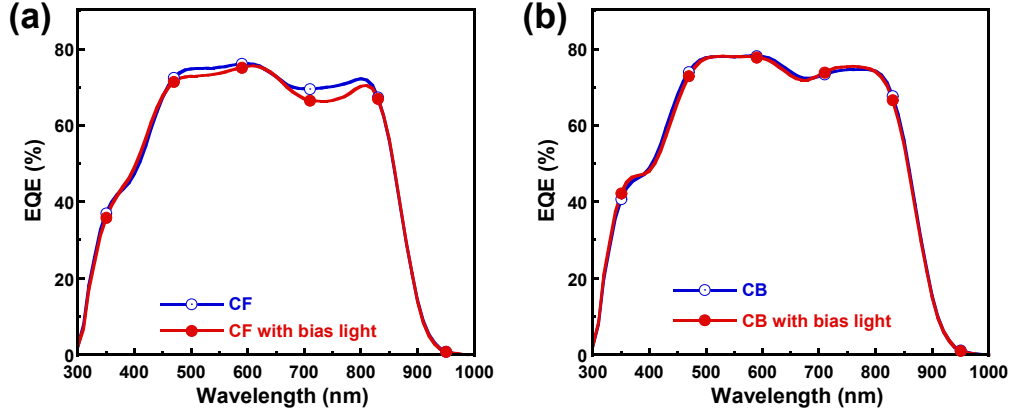
Fig. S6. EQE curves of PBDB-T:PFA1 devices processed by CF and CB with and without bias light.

Table S6. Average EQE$_{nobias}$/EQE$_{bias}$ and bimolecular recombination efficiency (η_{BR}) for PBDB-T:PFA1 devices processed by CF and CB.

Device	Average EQE$_{nobias}$/EQE$_{bias}$	Average bimolecular recombination efficiency (η_{BR}) [a]
CF	1.0213	2.13%
CB	1.0146	1.46%

[a] η_{BR} were calculated from the equation $\eta_{BR} = $ EQE$_{nobias}$/EQE$_{bias} - 1$

Table S7. Series resistance (R$_S$), shunt resistance (R$_P$), and the simulated ideality factor n for PBDB-T:PFA1 devices processed by CF and CB from dark J–V characteristics.

Device	R_S [a] (Ω cm^2)	R_P [a] (Ω cm^2)	n [b]
CF	1.20	8.33×10^3	1.85
CB	0.89	5.41×10^3	1.72

[a] R_S and R_P were calculated around 2 V and 0 V, respectively, from the dark J–V characteristics. [b] n was estimated by fitting of a one diode replacement circuit for the dark J–V characteristics.

Table S8. Calculated photovoltaic parameters for PBDB-T:PFA1 devices processed by CF (A) and CB (B).

Device	v_{oc}[b]	R_S^{*}[a] (Ω cm^2)	R_P^{*}[a] (Ω cm^2)	r_s[b]	r_p[b]	FF_0[b] (%)	FF_S[b] (%)	FF_{SP}[b] (%)
A	16.84	3.65	4.20×10^2	0.105	12.09	79.58	70.53	66.24
B	19.24	2.20	7.31×10^2	0.062	20.63	81.39	75.92	73.02

[a] R_S^{*} and R_P^{*} were obtained from illuminated J–V characteristics. [b] According to an equivalent circuit model reported by Kippelen et al., the upper-limit fill factor (FF_0), Rs-only-influenced fill factor (FF_S), and both Rs- and Rp- influenced fill factor (FF_{SP}) can be calculated as follows,

$$FF_0 = [v_{oc} - \ln(v_{oc} + 0.72)]/(v_{oc}+1),\ (R_S = 1/R_P = 0)$$

$$FF_S = FF_0\,(1 - 1.1\,r_s) + 0.19\,r_s^{2},\ (0 \leq r_s \leq 0.4,\ 1/r_p = 0)$$

$$FF_{SP} = FF_S\,[1 - (v_{oc} + 0.7)*FF_S/(v_{oc}*r_p)],\ (0 \leq r_s + 1/r_p \leq 0.4)$$

Where $v_{oc} = qV_{OC}/(nkT)$, q is the elementary charge, n is the ideality factor of the diode, and k is the Boltzmann's constant. r_s and r_p are normalized series and shunt resistance ($r_s = R_S *J_{SC}/V_{OC}$, $r_p = R_P* J_{SC}/V_{OC}$).
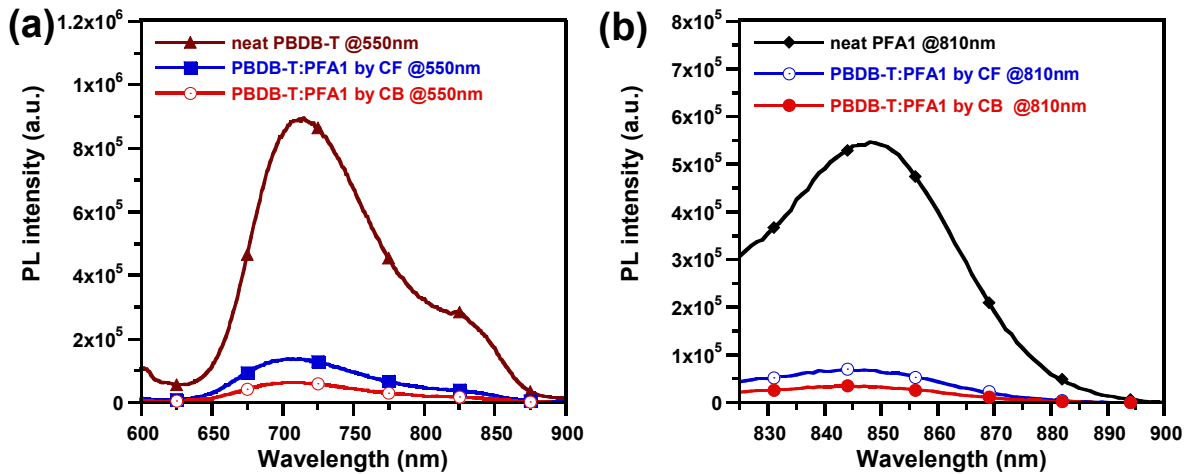

Fig. S7. PL spectra of neat PBDB-T, neat PFA1 and PBDB-T:PFA1 blends processed by CF and CB excited at (a) 550 nm and (b) 810 nm.

Table S9. Detailed GIWAXS (100) peak information in IP and (010) peak information in OOP of PBDB-T:PFA1 blend films processed by CF and CB.

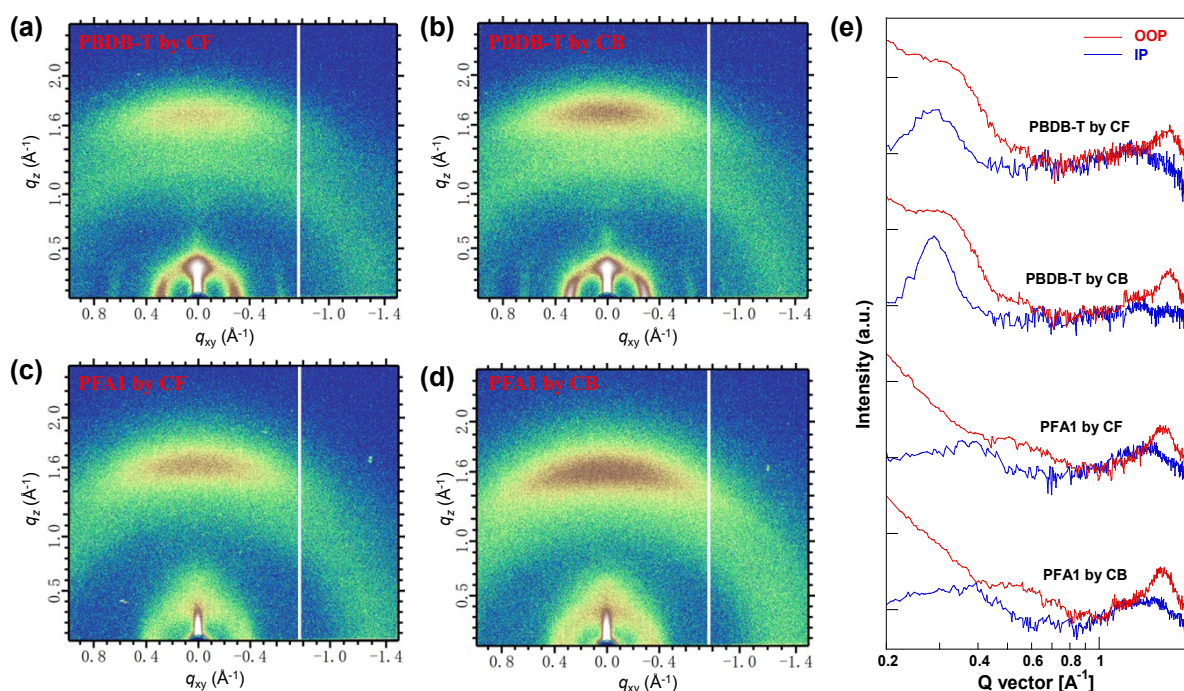| Solvent	Peak	Peak location (Å^{-1})	π-π stacking distance (Å)	FWHM (Å^{-1})	Lamellar stacking distance (nm)
CF	(100) in IP	0.29	/	0.15	4.20
	(010) in OOP	1.68	3.74	0.50	1.25
CB	(100) in IP	0.29	/	0.04	13.99
	(010) in OOP	1.72	3.65	0.42	1.50

Fig. S8. Two-dimensional grazing-incidence wide-angle X-ray scattering (GIWAXS) patterns (a-d) and one-dimensional integrated scattering profiles (e) for neat PBDB-T (neat PFA1) films processed by CF or CB.

Table S10. Detailed GIWAXS (100) peak information in IP and (010) peak information in OOP of neat PBDB-T (neat PFA1) films processed by CF or CB.

Film	Peak	Peak location (Å⁻¹)	π-π stacking distance (Å)	FWHM (Å⁻¹)	Lamellar stacking distance (nm)
neat PBDB-T by CF	(100) in IP	0.29	/	0.12	5.23
	(010) in OOP	1.70	3.69	0.65	0.96
neat PBDB-T by CB	(100) in IP	0.29	/	0.06	10.47
	(010) in OOP	1.72	3.65	0.40	1.57
neat PFA1 by CF	(100) in IP	0.34	/	0.31	2.03
	(010) in OOP	1.68	3.74	0.44	1.43
neat PFA1 by CB	(100) in IP	0.34	/	0.31	2.03
	(010) in OOP	1.68	3.74	0.43	1.46

References

1 F. Peng, K. An, W. Zhong, Z. Li, L. Ying, N. Li, Z. Huang, C. Zhu, B. Fan, F. Huang, Y. Cao, *ACS Energy Lett.*, 2020, **5**, 3702.